



Omnidirectional bandgap in Cantor dielectric multilayers

Francesco Chiadini^{a,*}, Vincenzo Fiumara^b, Ilaria Gallina^b, Antonio Scaglione^a

^a Department of Electrical and Information Engineering, University of Salerno, via Ponte Don Melillo, 84084 Fisciano, SA, Italy

^b Department of Environmental Engineering and Physics, University of Basilicata, Viale dell'Ateneo Lucano 10, 85100 Potenza, Italy

ARTICLE INFO

Article history:

Received 28 January 2009

Received in revised form 15 May 2009

Accepted 25 June 2009

PACS:

42.70.Qs

42.79.-e

42.79.Ci

Keywords:

Dielectric multilayers

Cantor fractals

Omnidirectional bandgap

ABSTRACT

Analysis of the transmission spectrum of Cantor dielectric multilayers for obliquely incident plane wave shows that the main bandgap shifts towards higher frequencies, substantially retaining its shape, as the incidence angle increases for both s- and p-polarization of the impinging wave. For suitable refractive index values of the two constituent materials a range of frequencies can be found where transmission of the incident wave is almost completely forbidden at any angle of incidence. This omnidirectional bandgap can be found also for lossy media. In this case the stop-band widens as the tangent loss increases, while the depth of the stop-band does not change significantly. Comparison with the periodic quarter-wave stack shows that the Cantor multilayer exhibits a narrower omnidirectional bandgap with transmissivity values that are about one order of magnitude lower.

© 2009 Elsevier B.V. All rights reserved.

1. Introduction

One dimensional periodic dielectric multilayers for which transmission of both p- and s-polarized light is forbidden for all incident angles and for a fairly wide range of wavelengths have been widely analyzed. In particular, it has been showed that when a plane electromagnetic wave propagates in a 1D periodic structure obliquely to the layer interfaces, the relative position of the bandgap is shifted towards higher frequencies while its width increases with the angle of incidence. As a result, if the refractive index values of the two dielectrics constituting the unit cell are properly chosen, a frequency band can be found where the incident wave is almost completely forbidden to propagate at any angle of incidence [1–4].

On the other hand, dielectric Cantor fractal multilayers have been extensively analyzed in the literature [5–8], but it has not been showed whether such systems can exhibit omnidirectional bandgap.

In this paper, we analyze the transmission properties of triadic Cantor multilayers for oblique incidence and show the existence of an omnidirectional bandgap for both polarization states, if suitable

refractive index values of the two materials, which the fractal multilayer consists of, are considered.

Moreover, we compare the omnidirectional bandgap characteristics of Cantor and periodic multilayers with the same (or closest to the same) number of layers, and the same refractive indexes of the two dielectric constituents.

The paper is organized as follows. In Section 2 Cantor multilayers are introduced. Their omnidirectional bandgap features are discussed in Section 3. Comparison between Cantor and periodic multilayers is reported in Section 4. Conclusions follow under Section 5.

2. Triadic Cantor multilayers

A triadic Cantor multilayer is a one dimensional structure with fractal morphology [9,10]. Generally, a fractal set can be obtained starting from a basic structure (initiator) and repeating *ad infinitum* a specific operation (generator) on smaller and smaller scales. Halting the generating process after a finite number of steps (stages of growth of the fractal) gives a prefractal which can be an appropriate model for physically realizable objects. Anyway, it is in the common use to adopt the term fractal for both prefractal and fractal sets. Henceforth we will conform to this terminology. In the case of the triadic Cantor construction the initiator is a segment and the generator consists in removing the dimension $1/R$ ($R > 1$) from the central part of all segments in the set. The

* Corresponding author. Tel.: +39 089 96 4281; fax: +39 089 96 4218.

E-mail addresses: fchiadini@unisa.it (F. Chiadini), vfiumara@unibas.it (V. Fiumara), ilaria.gallina@unibas.it (I. Gallina), ascaglione@unisa.it (A. Scaglione).

fractal at the stage of growth M is obtained by excising the dimension $1/R$ from the central part of all segments in the fractal at the stage $M - 1$. In the following we will confine to the case $R = 3$. The first four Cantor fractal stages are shown in Fig. 1. At the M -th stage of growth, the fractal set consists of 2^M segments separated by $2^M - 1$ gaps.

All segments have the same length L_M :

$$L_M = L/3^M \tag{1}$$

where L is the length of the initiator, while the length of the gaps depends on the stage at which they are created. The length ℓ_m of the 2^{m-1} gaps created at the m -th stage ($m = 1, \dots, M$) is:

$$\ell_m = L/3^m. \tag{2}$$

Cantor multilayers can be constructed by properly reformulating the procedure described above. At the generic M -th stage the multilayer is a succession of $N = 2^{M+1} - 1$ alternating, homogeneous layers of two dielectric materials with refractive indexes n_a and n_b , where layers n_a correspond to the segments of the Cantor set and layers n_b correspond to the gaps. Eqs. (1) and (2) give the optical length of the layers n_a and n_b , respectively. In this way, starting from the leftmost layer and progressively numbering the layers, their characteristics are as follows: odd layers (layer number, say, q) have refractive index n_a and thickness

$$d^{(q)} = d_a = \frac{L}{n_a 3^M}, \quad q \text{ odd} \tag{3}$$

while even layers have refractive index n_b and thickness

$$d^{(q)} = 3^{p-1} \frac{n_a d_a}{n_b}, \quad q \text{ even} \tag{4}$$

where p is the multiplicity of 2 in the prime factorization of q .

Consider a Cantor multilayer at the stage of growth M sitting between two semi-infinite dielectric media with refractive index n_{in} and n_{out} , and let a monochromatic planewave impinge on the multilayer with an angle θ_m with respect to the longitudinal axis of the structure. The transmission coefficient of the multilayer can be computed using the method of the characteristic matrixes along with the Snell's law at each interface [11]. Some papers [5–10] dealt with the analysis of transmission properties of Cantor multilayers for normal incidence. In this case the transmissivity of the multilayer exhibits several transparency/opacity windows. The deepest bandgap is bounded by two narrow transmission peaks and it is centered at:

$$f_0 = \frac{c}{4n_a d_a}, \tag{5}$$

c being the speed of light in vacuo.



Fig. 1. Triadic Cantor fractal set at different stages of growth.

3. Omnidirectional bandgap

As an example, we choose $n_a = 4.6$ and $n_b = 2.3$ as has been used in several papers [12–15]. Anyway, in this Section we also explain how the omnidirectional bandgap properties change with the indexes. Here and henceforth the stage of growth and the outer media are chosen to be $M = 3$ (number of layers $N = 15$), and $n_{in} = n_{out} = 1$, respectively. Note that there is no total reflection at any interface since $n_{in} < \min\{n_a, n_b\}$. Figs. 2 and 3 show the maps of the computed transmissivities for s- and p-polarization, respectively, as a function of both the normalized frequency f/f_0 and the angle of incidence. Like periodic dielectric multilayers [1–4], the transmissivity spectrum slightly shifts towards higher frequencies as the angle of incidence increases almost without changing its shape, regardless of the polarization. These figures show the existence of a range of frequency where transmission is forbidden (e.g., transmissivity less than 0.1) at any angle of incidence (omnidirectional bandgap) for both polarization states. To illustrate this to a greater extent Figs. 4 and 5 show the transmissivity spectrum at the angles of incidence $\theta_m = 0^\circ$ (solid line) and $\theta_m = 85^\circ$ (dotted line) for s- and p-polarization, respectively. The omnidirectional bandgap is the grey-highlighted area.

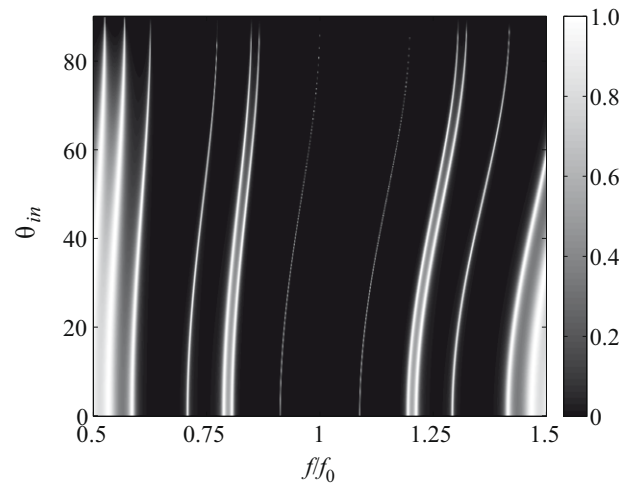


Fig. 2. Transmissivity spectrum of a triadic Cantor multilayer ($n_a = 4.6, n_b = 2.3, M = 3, n_{in} = n_{out} = 1$) as a function of the normalized frequency and of the angle of incidence (in degree) for an s-polarized incident plane wave.

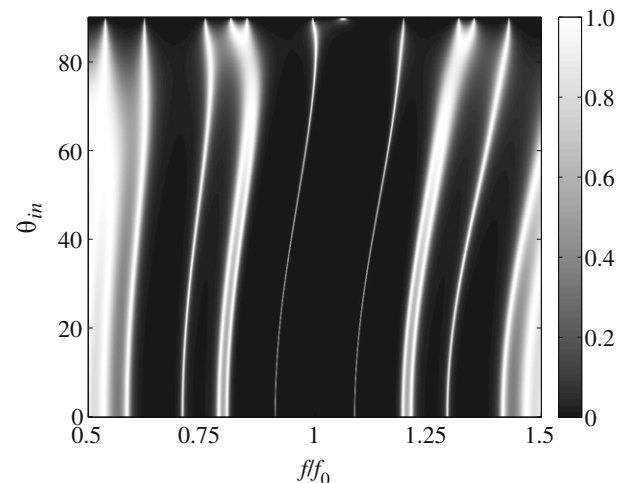


Fig. 3. Same as Fig. 2 but for a p-polarized plane wave.

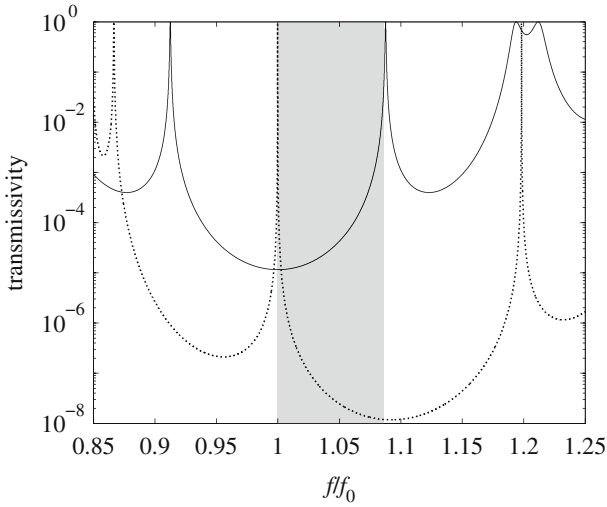


Fig. 4. Transmissivity spectra from Fig. 2 for angle of incidence $\theta_m = 0^\circ$ (solid line) and $\theta_m = 85^\circ$ (dotted line) as a function of the normalized frequency. The omnidirectional bandgap (transmissivity less than 0.1) is the grey-highlighted band.

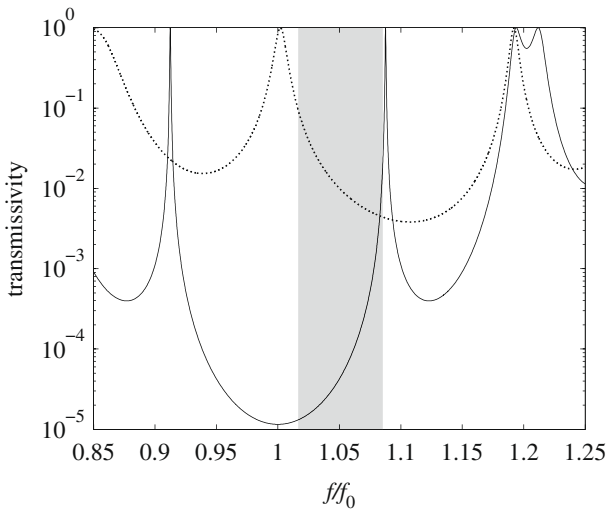


Fig. 5. Transmissivity spectra from Fig. 3 for angle of incidence $\theta_m = 0^\circ$ (solid line) and $\theta_m = 85^\circ$ (dotted line) as a function of the normalized frequency. The omnidirectional bandgap (transmissivity less than 0.1) is the grey-highlighted band.

The omnidirectional bandgap does not exist for any choice of the refractive indexes of the constituent media. That is illustrated in Figs. 6 and 7 where the relative width of the omnidirectional bandgap is plotted as a function of the refractive index n_a for various values of n_b . In particular, the figures show that, if the refractive index of one medium is assigned a value, say n_a , there is a threshold in the refractive index of the other medium, n_b . Moreover, the omnidirectional bandgap has a bandwidth that widens as n_a increases for both states of polarization.

As a further analysis, the existence of the omnidirectional bandgap has been investigated for dissipative media. As an example we use permittivities $\epsilon_a = n_a^2(1 - j \tan \delta)$ and $\epsilon_b = n_b^2(1 - j \tan \delta)$, with value of loss tangent $\tan \delta$ ranging from 10^{-6} up to 10^{-2} , and $n_a = 4.6$ and $n_b = 2.3$.

In Fig. 8 the value T_c of the depth of the stop-band is plotted as a function of the angle of incidence for a $\tan \delta = 10^{-6}$ (solid line) and $\tan \delta = 10^{-2}$ (dotted line). The figure shows that the depth of the stop-band is almost independent on the material dissipation.

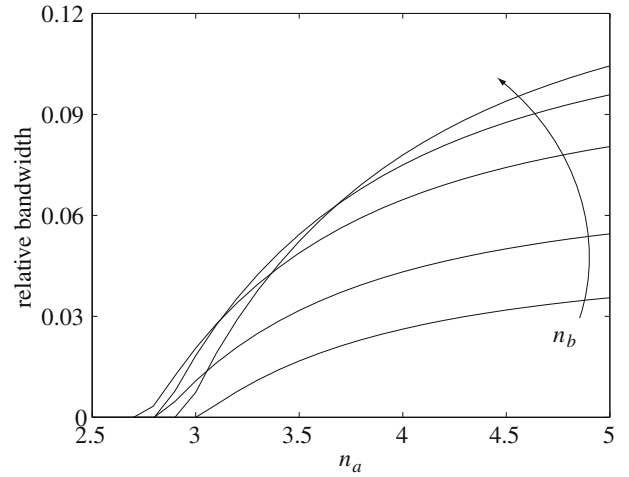


Fig. 6. Relative bandwidth of the omnidirectional bandgap as a function of the refractive index of the constituent media n_a for s-polarized planewave incidence. Lines are drawn for $n_b = 1.8, 1.9, 2.1, 2.3$ and 2.5 .

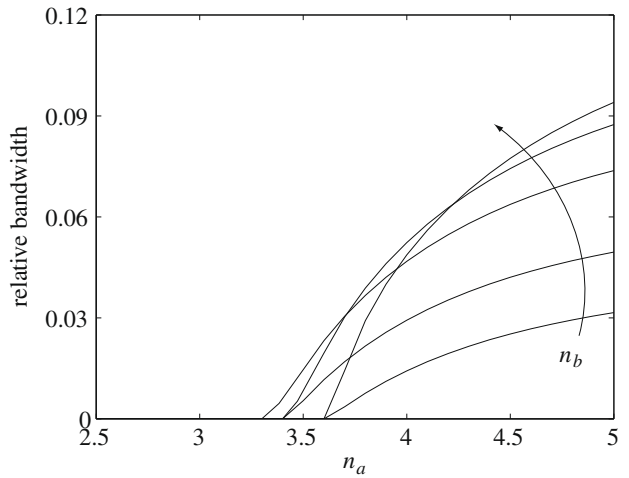


Fig. 7. Same as Fig. 6 but for p-polarized planewave incidence.

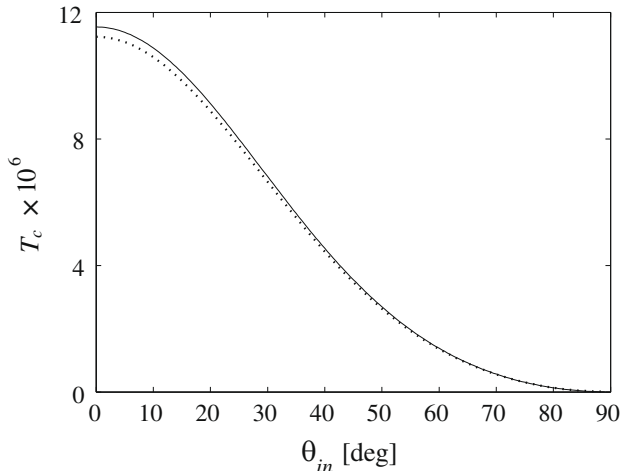


Fig. 8. Depth T_c of the stop-band as a function of the angle of incidence for $\tan \delta = 10^{-6}$ (solid line) and $\tan \delta = 10^{-2}$ (dotted line). s-polarized planewave incidence. $\epsilon_a = n_a^2(1 - j \tan \delta)$ and $\epsilon_b = n_b^2(1 - j \tan \delta)$ with $n_a = 4.6$ and $n_b = 2.3$.

In Fig. 9 the maximum transmissivity of the peak delimiting the right end of the stop-band is plotted as a function of the loss tangent for various values of the angle of incidence, $\theta_{in} = 0^\circ, 30^\circ, 60^\circ, 85^\circ$. For sake of brevity, only results for the right peak and s-polarization are reported since a similar behavior has been found for the left peak and p-polarization. In the Fig. 9 it can be seen that as long as $\tan \delta \leq 10^{-4}$ the transmissivity of the peak for any angle of incidence keeps higher than 0.1 that is the value below which we consider the wave transmission forbidden. Increasing $\tan \delta$ the maximum value of the right peak delimiting the stop-band becomes less than 0.1 at grazing angle of incidence resulting in an increment in the bandwidth of the omnidirectional bandgap. That is illustrated in Fig. 10 where the relative bandwidth of the omnidirectional bandgap is reported as a function of the loss tangent. It can be clearly seen that, for $\tan \delta \geq 10^{-4}$, the width of the omnidirectional bandgap begins to increase slightly because the maximum transmissivity of the peaks delimiting the stop-band becomes < 0.1 at lower and lower angles of incidence. When the loss tangent is higher than 10^{-3} the peaks have transmissivity < 0.1 already at normal incidence resulting in a steep increment in the omnidirectional bandwidth.

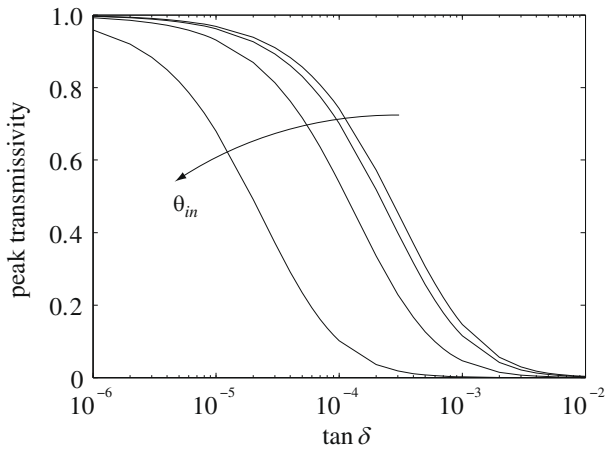


Fig. 9. Transmissivity of the right peak delimiting the stop-band as a function of the loss tangent for various values of the angle of incidence ($\theta_{in} = 0^\circ, 30^\circ, 60^\circ, 85^\circ$) and s-polarization. $\epsilon_a = n_a^2(1 - j \tan \delta)$ and $\epsilon_b = n_b^2(1 - j \tan \delta)$ with $n_a = 4.6$ and $n_b = 2.3$.

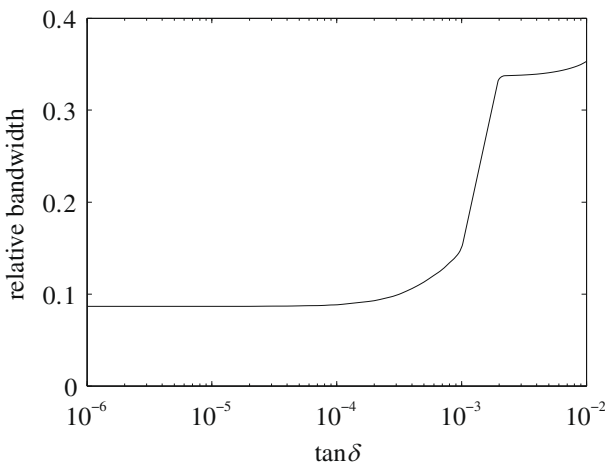
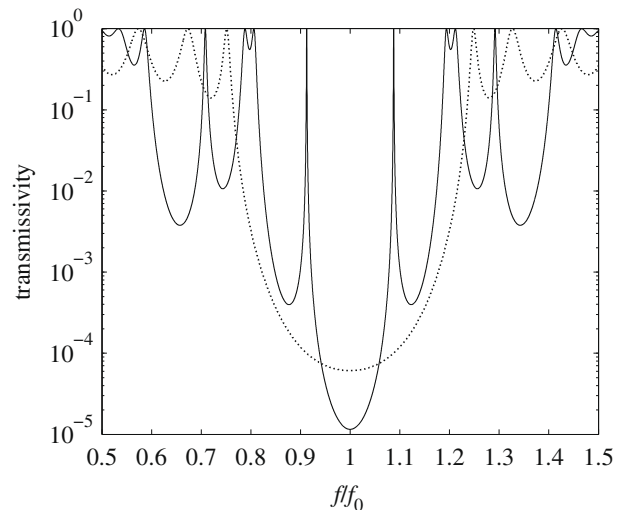


Fig. 10. Relative bandwidth of the omnidirectional bandgap as a function of the loss tangent for s-polarized planewave incidence. $\epsilon_a = n_a^2(1 - j \tan \delta)$ and $\epsilon_b = n_b^2(1 - j \tan \delta)$ with $n_a = 4.6$ and $n_b = 2.3$.

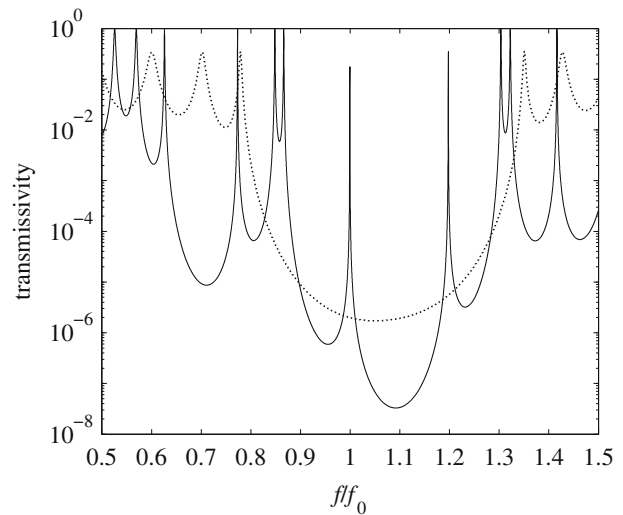
4. Comparison between Cantor and periodic omnidirectional bandgap

In order to draw a fair comparison between Cantor and periodic multilayers we consider a periodic multilayer with eight elementary cells, each consisting of two dielectric layers. Therefore, the number of layers in the analyzed Cantor and periodic structures are as close to the same as possible. The periodic stack has the same refractive indexes n_a and n_b as the Cantor multilayers, and it is also hosted in air. The thicknesses of the two layers in the elementary cell are $l_a = c/(4n_a f_0)$ and $l_b = c/(4n_b f_0)$, meaning that the elementary cell is half a wave thick at the frequency f_0 . For sake of brevity we show the results only for s-polarized wave.

As an example, let's compare the transmissivity spectra of the Cantor and periodic multilayer using $n_a = 4.6$ and $n_b = 2.3$. The spectra as a function of the normalized frequency are plotted in Fig. 11a for $\theta_{in} = 0^\circ$, and in Fig. 11b for $\theta_{in} = 85^\circ$. As it can be seen, the Cantor multilayer exhibits a transmissivity spectrum almost one order of magnitude lower than the one of the periodic



(a) $\theta_{in} = 0^\circ$



(b) $\theta_{in} = 85^\circ$

Fig. 11. Transmissivity spectra of Cantor multilayer (solid line) and of periodic multilayer (dotted line) as a function of the normalized frequency. Constituent materials of both structures are $n_a = 4.6$ and $n_b = 2.3$. s-polarized planewave incidence. (a) $\theta_{in} = 0^\circ$. (b) $\theta_{in} = 85^\circ$.

multilayer in the central frequency range of the main bandgap. The Cantor multilayer bandgap also turns out to be narrower than the bandgap of the periodic structure. These features have been observed for all the analyzed cases also for p-polarization, suggesting that a Cantor multilayer can be used to obtain an omnidirectional bandgap with lower transmissivity and narrower bandwidth than the periodic quarter-wave stack.

5. Conclusions

Transmissivity features of Cantor multilayers have been analyzed for either s-polarized and p-polarized obliquely incident planewave. It has been showed that the main bandgap shifts towards higher frequencies as the incidence angle increases. Furthermore, it has been showed that for both polarization states, if the media constituting the multilayer have suitable refractive index values, the structure exhibits an omnidirectional bandgap. For a given value of the refractive index of the less dense medium, the width of the omnidirectional bandgap widens when the refractive index of the other medium is increased.

The width of the omnidirectional bandgaps has been calculated also for lossy media. The main effect of the material dissipation is to decrease the maximum value of the peaks delimiting the stop-band and, consequently, to broaden the bandgap, while its depth does not change significantly.

Finally, we have drawn a comparison with periodic quarter-wave stacks showing that Cantor multilayers exhibit a narrower omnidirectional bandgap but with transmissivity values that are about one order of magnitude lower.

Acknowledgements

We thank an anonymous reviewer whose insightful comments lead to significant improvement of the presented work. This work has been sponsored in part by the Italian Ministry of Education, University and Research (PRIN 2006, Study and Realization of Metamaterials for Electronics and TLC applications).

References

- [1] J.N. Winn, Y. Fink, S. Fan, J.D. Joannopoulos, *Opt. Lett.* 23 (1998) 1573.
- [2] Y. Fink, J.N. Winn, S. Fan, C. Chen, J. Michel, J.D. Joannopoulos, E.L. Thomas, *Science* 282 (1998) 1679.
- [3] D.N. Chigrin, A.V. Lavrinenko, D.A. Yarotsky, S.V. Gaponenko, *Appl. Phys. A* 68 (1999) 25.
- [4] W.H. Southwell, *Appl. Opt.* 38 (1999) 5464.
- [5] A. Lakhtakia, K.E. Weaver, A. Verma, *Optik* 113 (2002) 510.
- [6] C. Sibilia, P. Masiulli, M. Bertolotti, *J. Opt. A-Pure Appl. Opt.* 7 (1998) 383.
- [7] F. Chiadini, V. Fiumara, I. Gallina, I.M. Pinto, A. Scaglione, *Opt. Commun.* 281 (2008) 633.
- [8] F. Chiadini, V. Fiumara, A. Scaglione, *J. Appl. Phys.* 100 (2006) 023119.
- [9] D.L. Jaggard, A.D. Jaggard, P.V. Frangos, *Fractal electrodynamics: surfaces and superlattices*, in: D.H. Werner, R. Mittra (Eds.), *Frontiers in Electromagnetics*, IEEE Press, 2000.
- [10] F. Chiadini, V. Fiumara, I.M. Pinto, A. Scaglione, *Microwave Opt. Technol. Lett.* 37 (2003) 339.
- [11] M. Born, E. Wolf, *Principles of Optics*, Cambridge, 1980.
- [12] G. Ouyang, Y. Xu, A. Yariv, *Opt. Express* 10 (2002) 899.
- [13] A.V. Lavrinenko, S.V. Zhukovsky, K.S. Sandomirski, S.V. Gaponenko, *Phys. Rev. E* 65 (2002) 036621.
- [14] X. Xu, G. Jin, Y. Ma, *Phys. Lett. A* 367 (2007) 360.
- [15] Y. Fink, D.J. Ripin, S. Fan, C. Chen, J.D. Joannopoulos, E.L. Thomas, *J. Lightwave Technol.* 17 (1999) 2039.